*Proceedings of the 11th Brazilian Congress of Thermal Sciences and Engineering -- ENCIT 2006*
*Braz. Soc. of Mechanical Sciences and Engineering -- ABCM, Curitiba, Brazil,- Dec. 5-8, 2006*

**Paper CIT06-0540**

# THEORETICAL MODEL FOR THE DISCHARGE PROCESS OF ADSORBED NATURAL GAS RESERVOIRS

**Luciano G. Lara**
Petrobras S/A – ENGENHARIA/IEABAST/EAB/ENPRO, Rio de Janeiro, RJ, 20031-004, Brazil
lglara@petrobras.com.br

**Paulo Couto**
Federal University of Rio de Janeiro – Petroleum Engineering – DEI/POLI, Rio de Janeiro, RJ, 21941-972, Brazil
pcouto@petroleo.ufrj.br

**Renato M. Cotta**
Federal University of Rio de Janeiro – PEM/COPPE, Rio de Janeiro, RJ, 21941-972, Brazil
cotta@serv.com.ufrj.br

**Dayse M. A. Sophia**
Federal University of Rio de Janeiro – PEM/COPPE, Rio de Janeiro, RJ, 21941-972, Brazil
dayse.sophia@gmail.com

***Abstract.*** *A model for the simulation of the discharge process of adsorbed natural gas reservoirs is presented. The objective of this work is to contribute to the development of a large-scale low-pressure reservoir vessel for adsorbed natural gas storage and transportation applications in Brazil. The complete derivation and analyses of the two-dimensional transient equations for energy, momentum and mass conservation are presented in this work. The derived equations are complete including convective terms. After solution, assumptions related to the slow discharge process are made to simplify the set of equations. Natural gas is modelled as pure methane, whose thermodynamic behaviour is modelled as ideal gas. The adsorption process is modeled according to Langmuir or Virial equation, depending on the adsorbent media considered inside the reservoir. The finite difference method was used to obtain a numerical solution for the model. Finaly, the results obtained with the presented model are compared to theoretical and experimental data available in the literature for validation purposes.*

***Keywords****. Natural Gas, Adsorption, Gas Transportation, and Gas Storage.*

## 1. Introduction

Natural gas is becoming an economically attractive fuel for many industrial applications in Brazil. However, the use of natural gas is still limited due, basically, to four factors: (1) conventional fuels, such as gasoline and diesel, are the most popular fuels in developed countries and they have been in use by internal combustion engines since its invention; (2) oil derivates have a large application in the chemical industry; (3) the energy density of Compressed Natural Gas – CNG (close to 11 MJ/Litre) is lower than that for liquid fuels (*e.g.*, energy density for gasoline is around 32 MJ/Litre); thus, (4) the storage and transportation of natural gas are not convenient when compared to conventional liquid fuels. When natural gas is in the gas phase, transportation occurs in gas pipelines and storage is performed in high-pressure cylinders, as CNG at pressure levels around 20 MPa. Although this technique provides storage capacity of 200 V/V (volume of stored natural gas at Standard Pressure and Temperature conditions – STP, per unit storage volume), it requires reliable and safe cylinders as well as costly compressing equipment. If the natural gas is in the liquid phase, as Liquefied Natural Gas – LNG, volumes as large as 600 V/V can be transported in ships and trucks. In this case, the gas must be cooled to temperatures as low as –160ºC. This technique is energetically expensive as heat leaks during transportation and storage vaporizes the LNG. Also, to be reused, the gas must be vaporized in appropriate equipment.

A new technology, however, has emerged as an alternative to CNG and LNG. It is known as Adsorbed Natural Gas – ANG (Burchell and Rogers, 2000; Litzke and Wegrzyn, 2001). Adsorption is the gas molecules uptake process in an interfacial layer (usually a highly porous media), whether by capillary condensation or by Van der Walls forces (Gregg and Sing, 1982). In the case of natural gas, the uptake process occurs at relatively low pressures, in the order of 3,5 to 5 MPa, which provides three main benefits: (1) compression costs reduction, (2) increased safety of the reservoir, and (3) design flexibility of the storage tanks. Despite these benefits, the storage capacity of ANG reservoirs is lower than LNG and CNG, being of the order of 90 V/V (Brady *et al*., 1996) up to 164 V/V (Inomata *et al*., 2002). The U.S. Department of Energy storage target for ANG vessels was set at 150 V/V and it was later revised to 180 V/V.

According to Biloé *et al*. (2002), the performance and viability of an ANG system depends closely on the microporous characteristics of the adsorbent as well as on the heat and mass transfer properties. The problems affecting ANG technology associated with the heat and mass transfer properties can be summarized as follows:

**1)** The adsorption phenomenon that occurs during the charge of an ANG reservoir is an exothermic process. The increase in temperature, caused by the release of latent heat of adsorption, results in less stored methane capacity under dynamic conditions (see Fig. 1 – left). During discharge of the ANG reservoir, the desorption process is endothermic,

which causes the adsorbent bed to cool down. This causes some amount of gas to be retained inside the reservoir at depletion pressure, reducing the delivered methane capacity (Fig. 1 – right). The thermal effects depend closely on the heat transfer properties of the adsorbent bed as well as on the external heat exchange at the vessel wall (Mota *et al.*, 1997 and Vasiliev *et al.*, 2000);

**2)** The high packing densities required for adsorbent beds (MacDonald and Quinn, 1998) create mass transfer limitations that limit the delivered and stored gas capacities (Mota *et al.*, 1997 and Biloé *et al.*, 2002).

The present work will focus on the complete theoretical derivation and analyses of the two-dimensional transient equations for energy, momentum and mass conservation. The derived equations are completed including convective terms. After solution, assumptions related to the slow discharge process are made to simplify the set of equations. Natural gas is modelled as pure methane, whose thermodynamic behaviour is modelled as ideal gas. The adsorption process is modelled according to Langmuir or Virial Equation, depending on the adsorbent media considered for the reservoir. The finite difference method was used to obtain a numerical solution for the model. Finally, for validation purposes, the results obtained with the presented model are compared to theoretical and experimental data available in the literature.

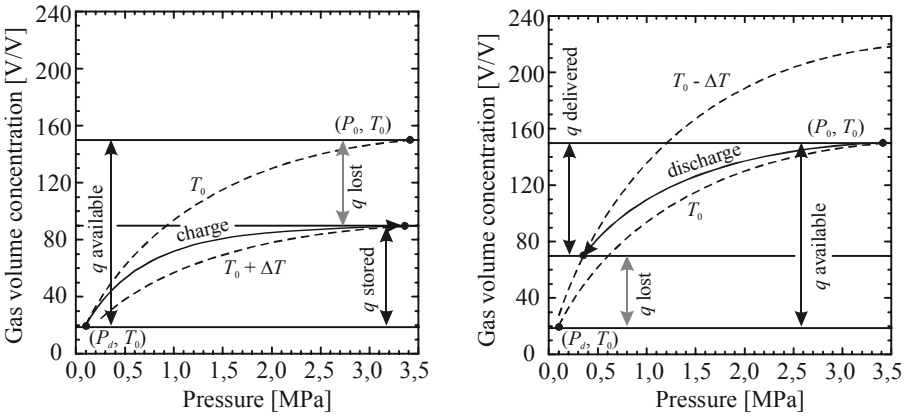


Figure 1. Charge (left) and discharge (right) processes of an ANG system.

## 2. Theoretical Analysis

Figure 2 shows the two-dimensional transient physical model analysed as an ANG reservoir. A cylindrical vessel of external radius $R_{ext}$ and length $L$, with a wall thickness of $\delta_w$ is considered. The gas flows outwards from the cylinder through a cylindrical opening of radius $R_0$ at the origin of the system, at a constant mass flow rate. Heat transfer by natural convection ($h_\infty$) between the external walls of the cylinder and the surroundings at $T_\infty$ is considered. The activated carbon bed is considered to be composed of activated carbon pellets with an effective porosity of $\varphi_{eff}$. Figure 2 also sketches the differential volume used for the derivation of the energy and mass balance equations. The volume has dimensions of $\Delta z$ by $\Delta r$, and is centred at the point ($z$, $r$). So, this differential volume has a volume given by $\Delta V = 2\pi r \Delta r \Delta z$. In the following sections, the mass continuity, energy balance and adsorption equilibrium relation are presented and discussed.

Mota *et al.* (1997) considered a carbon bed with activated carbon spheres with particle size of $R_p$ radius and porosity of $\varphi_p$. The packing density is given by $\rho_p$ and bed porosity by $\varphi$. In order to make easier the comprehension of following items, some assumptions are presented now. The subscripts ($s$), ($g$) and ($a$) will represent respectively solid, gas and adsorbed phases.

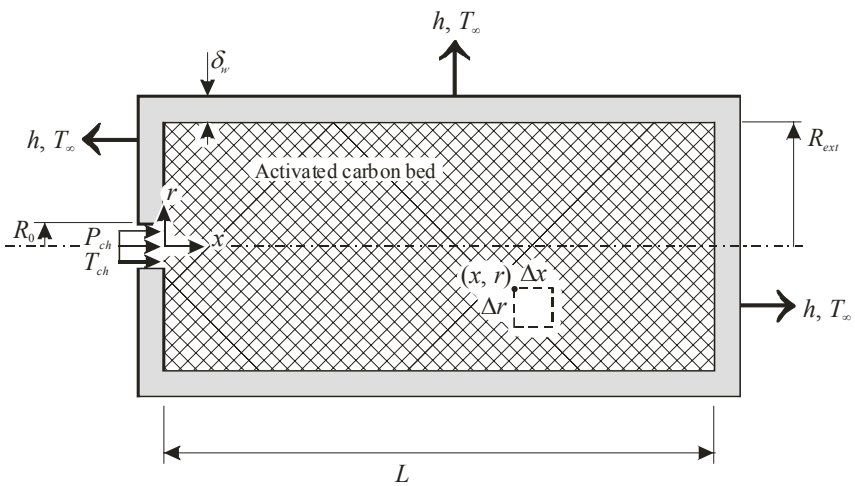


Figure 2. Physical model for the slow discharge process of an ANG reservoir.

### 2.2. Energy Balance in the Reservoir

The two-dimensional ($z$, $r$) energy equation presented here accounts for the contribution of the solid phase (adsorbent), gas phase (adsorbate), and the adsorbed phase in the total energy stored in the reservoir. Also, the contribution of the energy transfer by heat diffusion in the solid phase is considered. The latent heat of adsorption is considered as a rate of internal heat generation. The assumptions made for the energy conservation equation derivation are: (1) instantaneous phase equilibrium between the adsorbed phase and the gas phase within the porous structure, (2) the local temperature of the adsorbent and free gas volume is the same due to a high intensity heat transfer between solid and gas phases (Bejan, 1995). Also, (3) for the solid and adsorbed phases, the internal energy depends only on the local thermodynamic temperature (Moran and Shapiro, 2000) and (4) the adsorbed phase is considered incompressible (Tien, 1994). As the discharge process is considered to be slow, (5) the pressure gradient inside the cylinder is negligible (Mota *et al.*, 1997), *i.e*, the pressure is a function of time. Figure 3 shows the energy balance in the differential volume of Fig. 2.

Instantaneous phase equilibrium is assumed between the adsorbed phase and the gas phase within the porous structure, and the local temperature, say $T(z, r)$, of the adsorbent and free gas volume is the same due to a high heat transfer intensity between solid and gas phases (Nield and Bejan, 1992). For the differential control volume shown in Fig. 3, the first law of thermodynamics can be written as:

$$\left.\frac{\partial E}{\partial t}\right|_{CV} = \dot{Q}_{CV} - \dot{W}_{CV} + \left(\sum \dot{E}_{in} - \sum \dot{E}_{out}\right) \tag{1}$$

The left hand side of Eq. (1) can be written as:

$$\left.\frac{\partial E}{\partial t}\right|_{CV} = \left.\frac{\partial E'''}{\partial t}\right|_{CV} \Delta V = \left.\frac{\partial(\rho e)}{\partial t}\right|_{CV} \Delta V \tag{2}$$

where $E'''$ is the internal energy by unit volume, $\dot{E}$ is the energy flow at control volume faces and $e$ is the specific internal energy of each state is given by:

$$\left.\frac{\partial(\rho e)}{\partial t}\right|_{CV} \Delta V = \left(\varphi_{eff}\frac{\partial}{\partial t}(\rho_g e_g) + \frac{\partial}{\partial t}(\rho_s e_s) + \frac{\partial}{\partial t}(\rho_a e_a)\right) 2\pi r \Delta r \Delta z \tag{3}$$

According to Mota *et al.* (1997) the effective porosity $\varphi_{eff}$ of a porous bed made of compacted pellets of porosity $\varphi_p$, can be expressed by:

$$\varphi_{eff} = \varphi + (1-\varphi)\varphi_p \tag{4}$$

Considering that the energy conversion during the expansion or compression, $\dot{W}$, of the gas is negligibly small (Vasiliev *et al*. 2000), Eq. (1) can be rewritten as follows:

$$\left(\varphi_{eff}\frac{\partial}{\partial t}(\rho_g e_g) + \frac{\partial}{\partial t}(\rho_s e_s) + \frac{\partial}{\partial t}(\rho_a e_a)\right) 2\pi r \Delta r \Delta z = \left.\dot{Q}\right|_{CV} + (\dot{E}_{conv,in} - \dot{E}_{conv,out}) + (\dot{E}_{diff,in} - \dot{E}_{diff,out}) \tag{5}$$

The heat of adsorption can be expressed in terms of the latent (isosteric) heat of adsorption ($\Delta H$) and the rate of change of the adsorbed phase concentration ($\partial q/\partial t$), as follows (Tien, 1994):

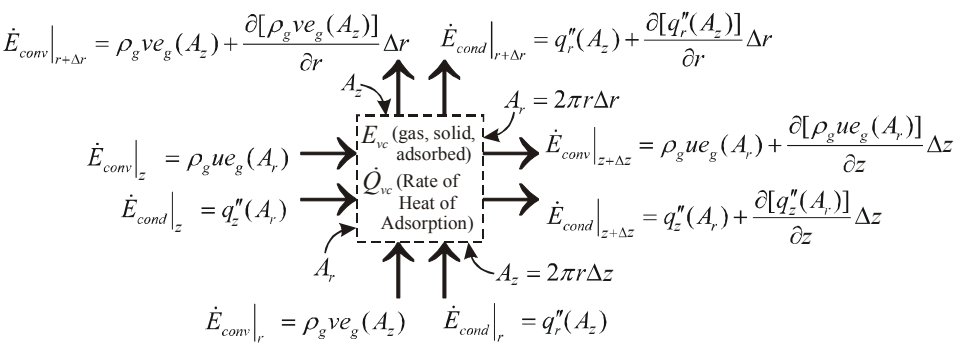


Figura 3: Energy balance for a GNA reservoir.

$$\dot{Q}\Big|_{CV} = \rho_s \Delta H \frac{\partial q}{\partial t}(2\pi r \Delta r \Delta z) \tag{6}$$

The balance of energy in the control volume by the fluid flow and heat diffusion can be written as follows:

$$\begin{aligned}\dot{E}_{conv,in} - \dot{E}_{conv,out} &= [\rho_g u e_g (2\pi r \Delta r) + \rho_g w e_g (2\pi r \Delta z)] + \\ &- \left\{ \rho_g u e_g (2\pi r \Delta r) + \frac{\partial[\rho_g u e_g (2\pi r \Delta r)]}{\partial z}\Delta z + \rho_g w e_g (2\pi r \Delta z) + \frac{\partial[\rho_g w e_g (2\pi r \Delta z)]}{\partial r}\Delta r \right\}\end{aligned} \tag{7}$$

$$\begin{aligned}\dot{E}_{diff,in} - \dot{E}_{diff,out} &= \{q''_z (2\pi r \Delta r) + q''_r (2\pi r \Delta z)\} + \\ &- \{[q''_z (2\pi r \Delta r) + \frac{\partial q''_z (2\pi r \Delta r)}{\partial z}\Delta z] + [q''_r (2\pi r \Delta z) + \frac{\partial q''_r (2\pi r \Delta z)}{\partial r}\Delta r]\}\end{aligned} \tag{8}$$

Equations (7) e (8) can be rewritten in order to obtain:

$$\dot{E}_{conv,in} - \dot{E}_{conv,out} = -\left( r\frac{\partial(\rho_g u e_g)}{\partial z} + \frac{\partial(r\rho_g w e_g)}{\partial r} \right) 2\pi \Delta r \Delta z \tag{9}$$

$$\dot{E}_{diff,in} - \dot{E}_{diff,out} = -\left( r\frac{\partial q''_z}{\partial z} + \frac{\partial(r q''_r)}{\partial r} \right) 2\pi \Delta r \Delta z \tag{10}$$

where $u$ and $w$ are the axial and radial velocity components respectively, and e $q_z''$ and $q_r''$ are the axial and radial components of the heat flux vector. Substituting Eqs. (6) to (10) in Eq. (5), one's obtain:

$$\varphi_{eff}\frac{\partial}{\partial t}(\rho_g e_g) + \frac{\partial}{\partial t}(\rho_s e_s) + \frac{\partial}{\partial t}(\rho_a e_a) = \rho_s \Delta H \frac{\partial q}{\partial t} - \left( \frac{\partial(\rho_g u e_g)}{\partial z} + \frac{1}{r}\frac{\partial(r\rho_g w e_g)}{\partial r} \right) - \left( \frac{\partial q''_z}{\partial z} + \frac{1}{r}\frac{\partial(r q''_r)}{\partial r} \right) \tag{11}$$

Some other assumptions are required now: 1) for the solid and adsorbed phases, the internal energy depends only on the local thermodynamic temperature (Moran and Shapiro, 2000 and Tien, 1994):

$$de_s = c_{p,s} dT \text{ ; and } de_a = c_{v,a} dT \tag{12}$$

2) The adsorbed phase is considered incompressible (Tien, 1994) and the specific heat of the adsorbed phase is approximately equal the specific heat of the gas ($c_{v,a} = c_{p,a}$):

$$c_{v,a} = c_{p,a} \cong c_{p,g} \tag{13}$$

3) As the adsorption process is superficial, the adsorbed phase density can be expressed in terms of solid phase density and adsorbed phase concentration (Tien, 1994):

$$\rho_a = \rho_s q \tag{14}$$

4) For the gas phase, the internal energy is written in terms of the enthalpy ($h_g$), density ($\rho_g$) and pressure ($P$):

$$h_g = e_g + P v_g \tag{15}$$

5) The Fourier law applies to the heat fluxes in the homogeneous porous bed:

$$q''_r = -k_{eff}\frac{\partial T}{\partial r} \text{ ; and } q''_z = -k_{eff}\frac{\partial T}{\partial z} \tag{16}$$

Therefore, Eq. (11) becomes:

$$\begin{aligned}&\varphi_{eff}\frac{\partial}{\partial t}(\rho_g h_g) - \varphi_{eff}\frac{dP}{dt} + \rho_s \frac{\partial}{\partial t}(c_{p,s}T) + \rho_s \frac{\partial}{\partial t}(c_{p,g} q T) = \rho_s \Delta H \frac{\partial q}{\partial t} + \\ &+ \left[ \frac{\partial}{\partial z}\left( k_{eff}\frac{\partial T}{\partial z} \right) + \frac{1}{r}\frac{\partial}{\partial r}\left( r k_{eff}\frac{\partial T}{\partial r} \right) \right] - \left( \frac{\partial(\rho_g u h_g - uP)}{\partial z} + \frac{1}{r}\frac{\partial(r\rho_g w h_g - rwP)}{\partial r} \right)\end{aligned} \tag{17}$$

The change in the gas phase specific enthalpy ($h_g$) can be expressed by the following thermodynamic relation:

$$dh_g = Tds_g + (1/\rho_g)dP \tag{18}$$

where $T$ is the absolute temperature and $ds_g$ the gas phase specific entropy change. As specific entropy is a function of $T$ and $P$, its variation is given by:

$$ds_g = \left(\frac{\partial s_g}{\partial T}\right)_P dT + \left(\frac{\partial s_g}{\partial P}\right)_T dP \tag{19}$$

From the Maxwell's relation (found in Moran and Shapiro, 2000), one's obtain:

$$\left(\frac{\partial s_g}{\partial T}\right)_P = \frac{c_{p,g}}{T}\text{; and } \left(\frac{\partial s_g}{\partial P}\right)_T = -\left(\frac{\partial(1/\rho_g)}{\partial T}\right)_P = \frac{1}{\rho_g^2}\left(\frac{\partial \rho_g}{\partial T}\right)_P = -\frac{\beta}{\rho_g} \tag{20}$$

Substituting the relations (20) in Eq. (19), provides:

$$ds_g = (c_{p,g}/T)_P dT - (\beta/\rho_g)dP \tag{21}$$

Equation (21) can be substituted in Eq. (18), resulting in:

$$dh_g = c_{p,g}dT + \frac{1}{\rho_g}(1-\beta T)dP \tag{22}$$

Equation (22) can be plugged in the first term on the left hand of Eq. (17):

$$\varphi_{eff}\frac{\partial}{\partial t}(\rho_g h_g) = \varphi_{eff}c_{p,g}\frac{\partial(\rho_g T)}{\partial t} + \varphi_{eff}(1-\beta T)\frac{dP}{dt} \tag{23}$$

Doing the same for the two last terms of right side of Eq. (17):

$$\frac{\partial(\rho_g u h_g)}{\partial z} = c_{p,g}\frac{\partial(\rho_g u T)}{\partial z} + (1-\beta T)\frac{\partial(uP)}{\partial z}\text{; and } \frac{\partial(r\rho_g w h_g)}{\partial r} = c_{p,g}\frac{\partial(r\rho_g w T)}{\partial r} + (1-\beta T)\frac{\partial(rwP)}{\partial r} \tag{24}$$

Rewriting Eq. (17) provides the following general form:

$$\begin{aligned}&\varphi_{eff}c_{p,g}\frac{\partial(\rho_g T)}{\partial t} + \rho_s\frac{\partial}{\partial t}(c_{p,s}T) + \rho_s\frac{\partial}{\partial t}(c_{p,g}qT) + \rho_s\Delta H\frac{\partial q}{\partial t} - \varphi_{eff}\beta T\frac{dP}{dt} - \beta T\left(\frac{\partial(uP)}{\partial z} + \frac{1}{r}\frac{\partial(rwP)}{\partial r}\right) = \\ &= \frac{\partial}{\partial z}\left(k_{eff}\frac{\partial T}{\partial z}\right) + \frac{1}{r}\frac{\partial}{\partial r}\left(rk_{eff}\frac{\partial T}{\partial r}\right) - c_{p,g}\left(\frac{\partial(\rho_g uT)}{\partial z} + \frac{1}{r}\frac{\partial(r\rho_g wT)}{\partial r}\right)\end{aligned} \tag{25}$$

For an ideal gas assumption, $\beta = 1/T$ (Bejan, 1995), Eq. (25) becomes:

$$\varphi_{eff}c_{p,g}\frac{\partial(\rho_g T)}{\partial t} + \rho_s\frac{\partial}{\partial t}(c_{p,s}T) + \rho_s\frac{\partial}{\partial t}(c_{p,g}qT) + \rho_s\Delta H\frac{\partial q}{\partial t} - \varphi_{eff}\frac{dP}{dt} - \nabla.(\mathbf{u}P) = \nabla.(k_{eff}\nabla T) - c_{p,g}\nabla.(\rho_g\mathbf{u}T) \tag{26}$$

In the equations (25) and (26), the three first terms on the left hand represent the thermal energy stored in the control volume by the gas, the solid and the adsorbed phases, respectively. The fourth term represents the heat of adsorption effects ($\Delta H$). The remaining terms on the left hand side represent the reversible portion of energy due to the gas compressibility effects. The terms on the right hand side of Eqs. (25) and (26), represent the diffusion and convection of heat within the activated carbon bed.

### 2.3. Mass Balance in the Reservoir

Figure 4 sketches the mass balance for the differential control volume shown in Fig. 2. The mass balance accounts for the net gas phase flow rate in the control volume, and the rate of phase change of the adsorbed and gas phases into the differential control volume. According to Fig. 4, the mass balance can be written as follows:

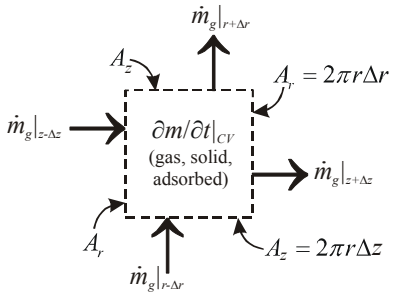


Figure 4: Mass balance for a GNA reservoir.

$$\left(\frac{\partial m_g}{\partial t}+\frac{\partial m_a}{\partial t}\right)\Bigg|_{CV}=\sum_{in}\dot{m}-\sum_{out}\dot{m} \tag{27}$$

The net mass flow rates in the control volume can be written as the product of the density, velocity and area:

$$\begin{aligned}\left(\frac{\partial(\varphi\rho_g\Delta V)}{\partial t}+\frac{\partial(\rho_a\Delta V)}{\partial t}\right)\Bigg|_{CV}&=\left[\rho_g u(2\pi r\Delta r)+\rho_g w(2\pi r\Delta x)\right]_{in}+\\ -\left[\rho_g u(2\pi r\Delta r)+\frac{\partial[\rho_g u(2\pi r\Delta r)]}{\partial x}\Delta x+\rho_g w(2\pi r\Delta x)+\frac{\partial[\rho_g w(2\pi r\Delta x)]}{\partial r}\Delta r\right]_{out}\end{aligned} \tag{28}$$

Equation (28) can be simplified by summing up the similar terms to provide:

$$\left(\varphi\frac{\partial\rho_g}{\partial t}+\frac{\partial\rho_a}{\partial t}\right)\Bigg|_{CV}\cancel{2\pi r\Delta r\Delta x}=-\left(\frac{\partial(\rho_g u)}{\partial x}+\frac{1}{r}\frac{\partial(r\rho_g w)}{\partial r}\right)\cancel{2\pi r\Delta r\Delta x} \tag{29}$$

From the third assumption [Eq. (14)], it follows that:

$$\varphi\frac{\partial\rho_g}{\partial t}+\rho_s\frac{\partial q}{\partial t}+\frac{\partial(\rho_g u)}{\partial x}+\frac{1}{r}\frac{\partial(r\rho_g w)}{\partial r}=0 \tag{30}$$

The ideal gas equation correlates $\rho_g$, $P$ and $T$.

### 2.4. Adsorption equilibrium relation (adsorption isotherms)

In almost all cases of adsorption, the parameters used in the adsorption equilibrium relation can be determined only from experimental data (Tien, 1994). Mota *et al.* (1997) presents the following experimentally obtained Langmuir equilibrium relation for the adsorption of methane in a G216 activated carbon bed:

$$\begin{aligned}&q=(q_m bP)/(1+bP)\\ &q_m=55920T^{-2.3}\,,\quad\text{and}\quad b=1{,}0863\times10^{-7}\exp(806/T)\end{aligned} \tag{31}$$

where $q$ is the adsorbed phase concentration, $P$ is pressure, and $T$ is temperature.

Chang and Talu (1996) presented a Virial form of the adsorption isotherms for the adsorption of methane in active carbon as follows:

$$P=qM_g\exp[(k_1+k_2/T)+(k_3+k_4/T)q] \tag{32}$$

where $M_g$ is the molecular weight of the gas, and $k_1$ to $k_4$ are temperature independent parameters determined by regression steps. For the case described by Chang and Talu (1996), the value for the constants are $k_1$ = 6,1317, $k_2$ = –2019,25, $k_3$ = 0,220956 and $k_4$ = 29,72837. Several other papers and works provide experimental data for the adsorption of natural gas in different compounds of activated carbons (Brady, 1996; Brady *et al.*, 1996; MacDonald and Quinn, 1998; and Ariyadejwanich *et al.*, 2003). These experimental data can be used for comparison with the different equilibrium relations presented here, or to derive new coefficients for these relations (Gregg and Sing, 1982).

**2.5. Slow Discharge Process**

The natural gas admission in a power cycle is controlled by power requirements of the system. In this case, discharge time is increased considerably by the slow rate of natural gas discharge, which usually occurs at a constant mass flow rate outward the cylinder at the opening (Mota *et al.*, 1997). The heat of adsorption during this process decreases the temperature of the adsorbent bed, which in turns, increases the amount of natural gas retained inside the cylinder at depletion (Biloé *et al.*, 2002). However, the discharge process is not adiabatic, and the heat transferred from the surroundings to the cylinder partially compensates this "cooling" effect. As the discharge process is considered to be slow, the pressure gradients inside the cylinder are negligible. This assumption leads to $u(t, x, r) = w(t, x, r) = 0$ during the slow discharge. Therefore, the energy equation is simplified to provide:

$$(\varphi_{eff} c_{p,g}\rho_g + \rho_s c_{p,s} + \rho_s c_{p,g} q)\frac{\partial T}{\partial t} + \rho_s \Delta H \frac{\partial q}{\partial t} - \varphi_{eff}\frac{d\overline{P}}{dt} = k_{eff}\nabla^2 T \tag{33}$$

The mass flow rate can be obtained by integrating the mass conservation equation (Eq. 30) in the entire cylinder domain ($0 \le z \le L$ e $0 \le r \le R_{ext}$):

$$0 = \int_0^L \left\{ \int_0^{R_{ext}} \left[ \varphi \frac{\partial \rho_g}{\partial t} + \rho_s \frac{\partial q}{\partial t} + \frac{\partial(\rho_g u)}{\partial x} + \frac{1}{r}\frac{\partial(r\rho_g w)}{\partial r} \right] 2\pi r dr \right\} dx \tag{34}$$

which can be expanded to:

$$0 = 2\pi \left\{ \int_0^L \int_0^{R_{ext}} \left[ \varphi \frac{\partial \rho_g}{\partial t} + \rho_s \frac{\partial q}{\partial t} \right] r dr dx + \int_0^{R_{ext}} r \int_0^L \left[ \frac{\partial(\rho_g u)}{\partial x} \right] dx dr + \int_0^L \int_0^{R_{ext}} \left[ \frac{\partial(r\rho_g w)}{\partial r} \right] dr dx \right\} \tag{35}$$

The first term on the right hand side of Eq. (35) represents the mass variation of natural gas, in the adsorbed and gas phases, inside the cylinder. The solution of the last two integrals provides the following relation:

$$0 = 2\pi \left\{ \frac{\partial}{\partial t} \int_0^L \int_0^{R_{ext}} (\varphi\rho_g + \rho_s q) r dr dx + \int_0^{R_{ext}} r \left[ \rho_g u \right]_{x=0}^{x=L} dr + \int_0^L \left[ r\rho_g w \right]_{r=0}^{r=R_{ext}} dx \right\} \tag{36}$$

The last integral vanishes, once $w = 0$ at $r = 0$ and at $r = R_{ext}$. The velocity component $u$ at $x = 0$ has two values: (1) for $0 \le r \le R_0$, the gas leaving the cylinder has a constant velocity determined by the constant mass flow rate ($u = u_{ch}$); (2) for $R_0 < r \le R_{ext}$, $u = 0$ at the cylinder wall. Also, at $x = L$, $u = 0$. Therefore, the second term can be split in two integrals, as follows:

$$0 = 2\pi \left\{ \frac{\partial}{\partial t} \int_0^L \int_0^{R_{ext}} (\varphi\rho_g + \rho_s q) r dr dx + \int_0^{R_0} r \left[ \rho_g u \right]_{x=0}^{x=L} dr + \int_{R_0}^{R_{ext}} r \left[ \rho_g u \right]_{x=0}^{x=L} dr \right\} \tag{37}$$

The last integral vanishes, as $u = 0$ at $x = 0$ and at $x = L$ for $R_0 < r \le R_{ext}$. The argument of the second integral becomes ($-\rho_{g,ch}u_{ch}$) as $u = 0$ at $x = L$, and $u = u_{ch}$ at $x = 0$ for $0 \le r \le R_0$. So, Eq. (37) becomes:

$$2\pi \frac{\partial}{\partial t} \int_0^L \int_0^{R_{ext}} (\varphi\rho_g + \rho_s q) r dr dx = \int_0^{R_0} \rho_{g,ch} u_{ch} 2\pi r dr \tag{38}$$

The right hand side of Eq. (38) represents the mass flow rate ($\dot{m}$) leaving the cylinder at $x = 0$ and $0 \le r \le R_0$. Therefore, the final form of the mass conservation equation is obtained:

$$2\pi \frac{d}{dt} \int_0^L \int_0^{R_{ext}} (\varphi\rho_g + \rho_s q) r dr dx = \dot{m} \tag{39}$$

The solution of the discharge model is iterative. Equation (39) can be used to determine the gas phase pressure, $P$, provided a constant mass flow rate for the discharge process. The energy equation (33) can be used to obtain the temperature distribution inside the cylinder. Then, the state equation is used to obtain the gas phase density, $\rho_g$, and the adsorbed gas concentration is obtained from the equilibrium relation (31) or (32).

### 2.6. Initial and Boundary Conditions

Initial conditions are required for temperature and pressure, and boundary conditions are required only for the temperature. At the beginning of the discharge process, the cylinder is considered to be at a homogeneous and uniform temperature and pressure, $T_1$ and $P_{ch}$ (the subscript 1 is used to distinguish the slow discharge initial condition for energy equation from the fast charge initial condition). The initial and boundary conditions are given as follows:

$$T(0,x,r) = T_1 \tag{40}$$

$$P(0) = P_{ch} \tag{41}$$

$$\left.\frac{\partial T}{\partial x}\right|_{x=0} = 0\,, \qquad \text{at } x = 0, \text{ for } t > 0 \text{ and } 0 \le r \le R_0 \tag{42}$$

$$-k_{eff}\left.\frac{\partial T}{\partial x}\right|_{x=0} + \rho_w c_{p,w}\delta_w \left.\frac{\partial T}{\partial t}\right|_{x=0} = h(T_\infty - T|_{x=0})\,, \qquad \text{at } x = 0, \text{ for } t > 0 \text{ and } R_0 < r \le R_{ext} \tag{43}$$

$$k_{eff}\left.\frac{\partial T}{\partial x}\right|_{x=L} + \rho_w c_{p,w}\delta_w \left.\frac{\partial T}{\partial t}\right|_{x=L} = h(T_\infty - T|_{x=L})\,, \qquad \text{at } x = L, \text{ for } t > 0 \text{ and } 0 < r \le R_{ext} \tag{44}$$

$$k_{eff}\left.\frac{\partial T}{\partial r}\right|_{r=R_{ext}} + \rho_w c_{p,w}\delta_w \left.\frac{\partial T}{\partial t}\right|_{r=R_{ext}} = h(T_\infty - T|_{r=R_{ext}})\,, \qquad \text{at } r = R_{ext}, \text{ for } t > 0 \text{ and } 0 < x \le L \tag{45}$$

$$\left.\frac{\partial T}{\partial r}\right|_{r=0} = 0\,, \qquad \text{at } r = 0, \text{ for } t > 0 \text{ and } 0 < x \le L \tag{46}$$

Although gas leaves the cylinder, it is considered that the discharge occurs isothermally at the opening (Vasiliev *et al.*, 2000). Boundary condition (42) accounts for this assumption. The cylinder walls thermal capacity is included in boundary conditions (43) to (45) as well as the heat transferred to the system by the thermal control device [boundary condition (46)]. The external wall heat transfer coefficient, $h$, can be obtained from classical correlation for natural convection in horizontal cylinders (Bejan, 1995).

### 2.6. Solution Methodology

A numerical approach based on the finite difference method was used to obtain an approximate solution for the model. Equations (33), (39) and (40) to (46) were discretized using a fully implicit formulation, with centred differences for the diffusion terms. The discretized version of equation (39) is:

$$\left[\sum_{i=1}^{I}\sum_{j=1}^{J}(\varphi_{eff}\rho_{g,[i,j]} + \rho_s q_{[i,j]})\Delta V_{[i,j]} - \sum_{i=1}^{I}\sum_{j=1}^{J}(\varphi_{eff}\rho^0_{g,[i,j]} + \rho_s q^0_{[i,j]})\Delta V_{[i,j]}\right]\Delta t^{-1} = \dot{m} \tag{47}$$

where $i$ and $j$ are indexes for the discretization in the $z$ and $r$ directions respectively, $I$ and $J$ are total number of nodes in the $z$ and $r$ directions, and the superscript "0" indicates the previous time step values. The *Mathematica 4.2* software was used for the solution of the model's equations. To control the convergence of the solution a successive over-relaxation method was used with a relaxation coefficient equal to 0.5. The solution is iterative and proceeds as follows:

1. Based on the initial conditions, $\rho^0_{[i,j]}$ and $q^0_{[i,j]}$ are calculated and the time step is increased by $\Delta t$;
2. The estimative of pressure is calculated from equation (47) based on the last temperature distribution available;
3. Estimates for $\rho_{[i,j]}$ and $q_{[i,j]}$ are calculated based on $P$ and the estimative for the temperature distribution $T_{[i,j]}$ is calculated from the discretized version of Eq. (33);
4. The convergence criterion for pressure and temperature are checked and steps 2 through 4 are repeated successively until convergence is achieved;
5. Once convergence is achieved, $P$, $T_{[i,j]}$, $\rho_{[i,j]}$ and $q_{[i,j]}$ are stored, the initial boundary conditions for the next time step are updated, and steps 1 through 5 are repeated until the pressure inside the reservoir achieves a given depletion pressure $P_d$. The convergence criterion used in this work compares the variation of the results for temperature and pressure for two consecutives iterations, as follows:

$$\varepsilon^T_{\max} \ge Max\left[Abs\left(\frac{T_{[i,j]} - T^k_{[i,j]}}{T_{[i,j]}}\right)\right]\times 100 \quad \text{and} \quad \varepsilon^P_{\max} \ge Max\left[Abs\left(\frac{P - P^k}{P}\right)\right]\times 100 \tag{48}$$

where $\varepsilon^T_{max}$ and $\varepsilon^P_{max}$ are the maximum tolerances for temperature and pressure, respectively. Convergence analyses were performed by the authors to determine the optimum values for $\varepsilon^T_{max}$, $\varepsilon^P_{max}$, $\Delta z$, $\Delta r$, and $\Delta t$ (Lara, 2005).

## 3. Model Validation

For the model validation, two sets of data were used (Chang and Talu, 1996 and Mota *et al*., 1997). The parameters used for the model validation are shown in Table 1. Chang and Talu (1996) presented a theoretical and experimental analysis of the slow discharge process. They experimentally tested a 23,2 litres cylinder, which was instrumented with four thermocouples at different radial positions and at the cylinder wall. Also, the gas pressure inside the cylinder was monitored. Chang and Talu (1996) presented a one-dimensional transient theoretical analysis of the slow discharge of the tested ANG vessel. Their model did not consider the gas compressibility effects either the contribution of the gas and adsorbed phases in the energy stored inside the cylinder. The pressure history was determined by the solution of the mass conservation equation. The effect of the cylinder wall was taken into account in the wall boundary condition ($r = R_{ext}$). Figure 5 shows the comparison of the pressure history inside the cylinder obtained with the present model and the experimental data of Chang and Talu (1996). The radial temperature distribution obtained with the presented model and the experimental data presented by Chang and Talu (1996) is shown in Figure 6. The comparison between the presented model and experimental data is good and the current simulation was able to capture the pressure transient and the temperature gradient trends of the slow discharge process. The differences between the data resulting from the presented model and the experimental data presented by Chang and Talu (1996) can be attributed to the poor discussion on the experimental conditions (heat transfer coefficient on the external wall) presented by Chang and Talu (1996).

Table 1. Parameters used for model validation.

| **Author:** | **Chang & Talu (1996)** | | **Mota *et al.* (1997)** | |
|---|---|---|---|---|
| *Activated carbon bed properties:* | | | | |
| Type | N/A | | G216 carbon pellets | |
| Density – $\rho_s$ | 975,0 | kg/m$^3$ | 410,0 | kg/m$^3$ |
| Specific heat – $c_{p,s}$ | 1052,0 | J/kg.K | 650,0 | J/kg.K |
| Effective conductivity – $k_{eff}$ | 0,212 | W/m.K | 1,2 | W/m.K |
| Effective porosity – $\varphi_{eff}$ | 0,5 | | 0,74 | |
| *Cylinder geometry:* | | | | |
| Material | Stainless steel | | Stainless steel | |
| Density – $\rho_w$ | 7800,0 | kg/m$^3$ | 7900,0 | kg/m$^3$ |
| Specific heat – $c_{p,w}$ | 502,6 | J/kg.K | 496,2 | J/kg.K |
| External radius – $R_{ext}$ | 0,1 | m | 0,14 | m |
| Length – $L$ | 0,74 | m | 0,85 | m |
| Inlet radius – $R_0$ | 0,00476 | m | 0,005 | m |
| Thickness – $\delta_w$ | 0,0055 | m | 0,01 | m |
| *Operational conditions:* | | | | |
| Initial pressure [MPa] | 2,1 | MPa | 3,5 | MPa |
| Depletion pressure [MPa] | 166,0 | kPa | 101,325 | kPa |
| Initial temperature [K] | 291,0 | K | 285,0 | K |
| Ambient temperature [K] | 291,0 | K | 285,0 | K |
| Flow rate | 6,7 | L/min | 0,018 | kg/min [(2)] |
| *Adsorption characteristics:* | | | | |
| Equilibrium relation | Virial equation | | Langmuir equation | |
| Heat of adsorption | $\Delta H = f(R_g, q)$ | | $\Delta H = -1{,}1 \times 10^6$ J/kg | |

[1] Matrix made of Expanded Natural Graphite (ENG) and Superactivated Carbon (Maxsorb).
[2] Value inferred from performance coefficient data provided by Mota *et al.* (1997).

Mota *et al.* (1997) presented a one-dimensional transient theoretical analysis of the slow discharge of a 50 litres ANG cylinder, were emphasis was given to thermal and mass diffusion effects in the activated carbon bed. Natural gas was modelled as ideal gas pure methane. Although these authors presented a complete energy equation, the pressure history was imposed, and not determined by the mass conservation equation. The imposed pressure history led to a constant mass flow rate at the cylinder outlet. Figure 7 shows the comparison of the radial temperature profile obtained in this work and the theoretical data obtained by Mota *et al.* (1997). The comparison between the current and Mota *et al.* (1997) analyses is fair, and the presented model was able to reproduce the same radial temperature gradient trends. Figure 8 shows the comparison between the performances coefficient obtained with the current analysis and the data presented by Mota *et al.* (1997) as a function of discharge time. The performance coefficient is defined as the ratio between the real mass of methane delivered and the mass of methane delivered if the discharge process was isothermal:

$$\eta = \frac{m_{delivered,real}}{\{[\varphi_{eff}\rho_g(T_0,P_0)+\rho_s q(T_0,P_0)]-[\varphi_{eff}\rho_g(T_0,P_f)+\rho_s q(T_0,P_f)]\}V_{cylinder}} \tag{49}$$

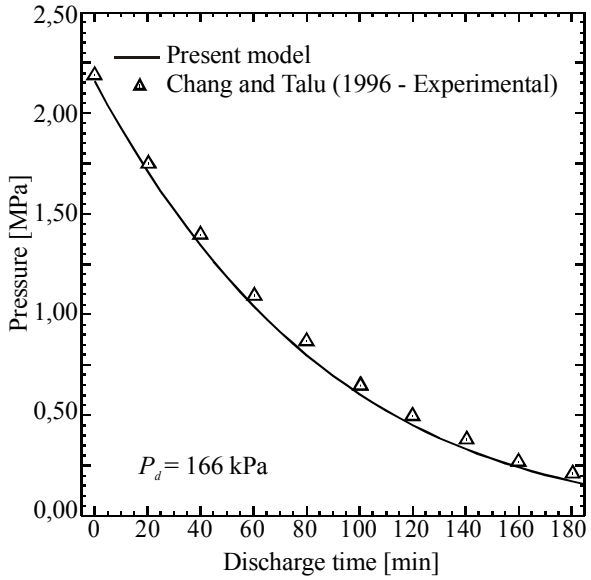


Figure 5: Comparison of pressure history (Chang and Talu., 1996)

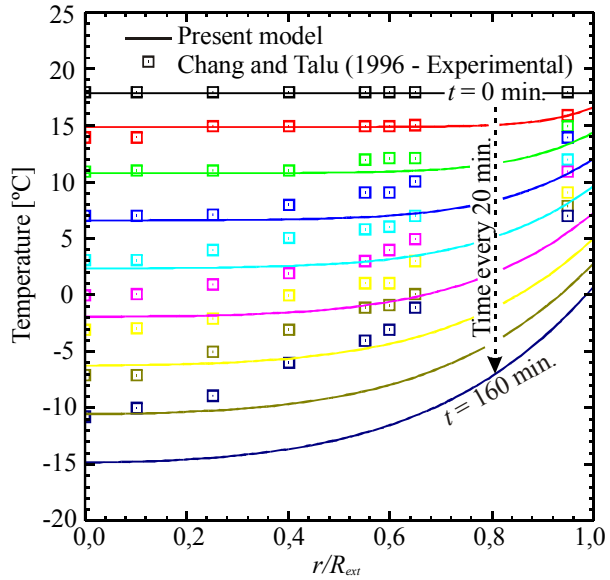


Figure 6: Comparison of radial temperature distribution (Chang and Talu., 1996)

The authors of the present work believe that the methodology used in the current model to determine the pressure history is more physically consistent than the methodology used by Mota *et al*. (1997). The power requirement of a given system (*e.g.*, internal combustion engine) controls the consumption of fuel, thus imposing a mass flow rate at the outlet of the reservoir. This hypothesis is mathematically modeled by Eq. (39). To impose a pressure history to the reservoir, a pressure control valve would be required at the outlet, which is not the usual case. The differences in the theoretical data obtained with this model and the theoretical data presented by Mota *et al*. (1997) is due to this methodology difference. Figure 9 shows the influence of discharge time on the cylinder temperature radial profile at the end of each discharge process with different flow rates. The fast discharge does not increase the quantity of discharged mass for the reason that the temperature gradient is higher due the low rate of heat diffusion, taking to lower temperatures.

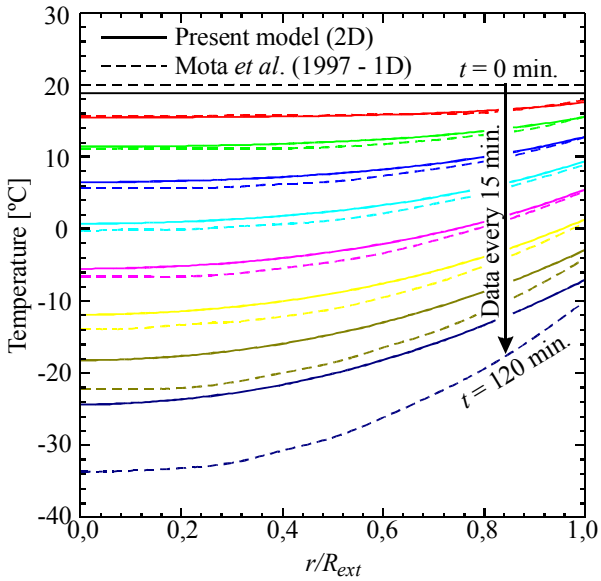


Figure 7: Comparison of radial temperature distribution (Mota *et al*., 1997)

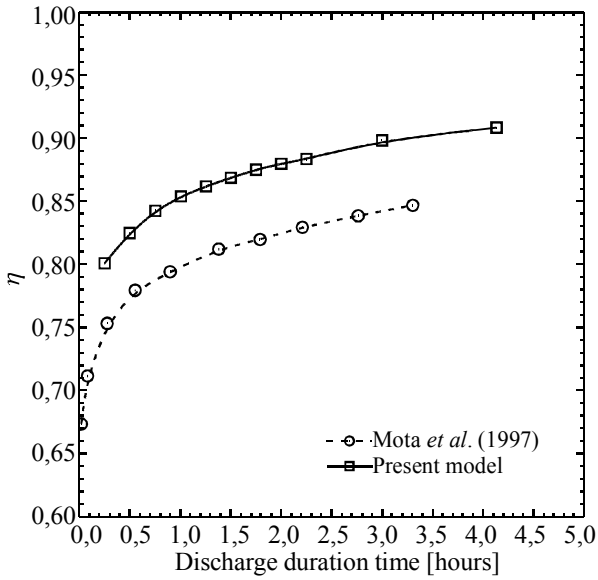


Figure 8: Comparison of performance coefficient (Mota *et al*., 1997)

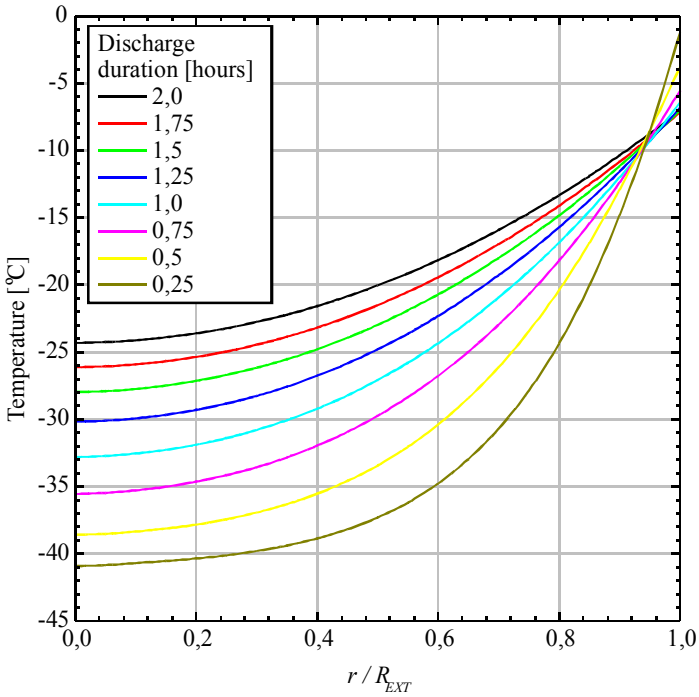


Figure 9: Final Radial Temperature Profile for discharge times.

## 4. Conclusion

A two-dimensional model for the slow discharge process was presented and discussed. The derivation of energy balance, mass continuity and adsorption equilibrium relation equations referring to mathematical modelling, the thermodynamic and physical conditions that involves the natural gas discharge process in cylindrical reservoir as well the assumptions were presented and discussed. The validation using Mota *et al.* (1997) data was satisfactory, as the data obtained by model showed the same trends of the theoretical data obtained by these authors. The differences between the two models are attributed to the method Mota *et al*. (1997) determined the pressure profile. The validation of the model showed that the methodology presented here is in agreement with the physics of the slow discharge process. In order to make a rigorous validation, the results obtained by the present model were compared to the experimental data presented by Chang and Talu (1996). The comparison between pressure profiles was satisfactory for the validation of the pressure calculation method of the present work. For the temperature profiles, the results showed the same trends, although Chang and Talu did not present consistent information about the values of some experimental parameters, such as the convection heat transfer coefficient they used.

## 5. Nomenclature

| | |
|---|---|
| $c_p$ | Isobaric heat capacity |
| $h_f$ | Forced convection heat transfer coefficient |
| $h_\infty$ | Natural convection heat transfer coefficient |
| $k_{eff}$ | Effective thermal conductivity |
| $L$ | Cylinder length |
| $\dot{m}$ | Mass flow rate |
| $P$ | Pressure |
| $P_d$ | Depletion pressure |
| $q$ | Adsorbed phase concentration |
| $R_0$ | Cylinder filling opening radius |
| $R_{ext}$ | Cylinder external radius |
| $r$ | Radial coordinate |
| $T$ | Temperature |
| $T_\infty$ | Surrounding temperature |
| $t$ | Time |
| $V$ | Volume |
| $z$ | Axial coordinate |

**Greek Symbols:**

| | |
|---|---|
| $\Delta H$ | Latent (isosteric) heat of adsorption |
| $\varepsilon^P_{max}$ | Max. tolerance for pressure convergence |
| $\varepsilon^T_{max}$ | Max. tolerance for temperature convergence |
| $\delta_w$ | Cylinder wall thickness |
| $\varphi_{eff}$ | Effective porosity |
| $\rho$ | Density |

**Subscripts:**

| | |
|---|---|
| $(\ )_a$ | Adsorbed phase |
| $(\ )_g$ | Gas phase |
| $(\ )_s$ | Solid phase |
| $(\ )_w$ | Cylinder wall properties |
| $(\ )_0$ | Initial condition |

## 6. Acknowledgement

The authors would like to acknowledge CNPq for funding this research. Luciano G. Lara would like to acknowledge Petrobras S/A – ENGENHARIA/IEABAST/EAB/ENPRO for supporting this work.

## 7. References

Ariyadejwanic, P.; Tanthapanichakoon, W.; Nakagawa, K.; Mukai, S. R.; and Tamon, H., 2003. "Preparation and Characterization of Mesoporous Activated Carbon from Waste Tires". In: *Carbon*, Vol. 41, pp. 157-164.

Bejan, A., 1995. **Convection Heat Transfer**. 2nd Ed., New York, NY: John Wiley & Sons, Inc.

Biloé, S.; Goetz, V.; and Mauran, S., 2001. "Dynamic Discharge and Performance of a New Adsorbent for Natural Gas Storage". In: *AIChE Journal*, Vol. 47, no. 12, pp. 2819-2830.

Brady, T. A.; Rostam-Abadi, M.; and Rood, M. J., 1996. "Applications for Activated Carbons from Waste Tires: Natural Gas Storage and Air Pollution Control". In: *Gas Separation and Purification*, Vol. 10, no. 10, pp. 97-102.

Burchell, T. and Rogers, M., 2000. "Low Pressure Storage of Natural Gas for Vehicular Applications". SAE Tech. Paper Series no. 2000-01-2205, In: Government/Industry Meeting, Washington, D.C.

Chang, K. J. and Talu, O., 1996. "Behavior and Performance of Adsorptive Natural Gas Storage Cylinders During Discharge". In: *Applied Thermal Engineering*, Vol. 16, no. 5, pp. 359-374.

Gregg, S. J. and Sing, K. S. W., 1982. **Adsorption, Surface Area and Porosity.** 2nd ed., London: Academic Press, Inc.

Inomata, K.; Kanazawa, K.; Urabe, Y.; Hosono, H. and Araki, T., 2002. "Natural gas storage in activated carbon pellets without a binder". In: *Carbon*, Vol. 40, pp. 87-93.

Lara, L.G., 2005. **Theoretical Analysis of the Discharge Process of Adsorbed Natural Gas Reservoirs** (*original in Portuguese*). M. Sc. thesis, Mech. Eng. Programme, Fed. Univ. of Rio de Janeiro, Brazil.

Litzke, W. L. and Wegrzyn, J., 2001. "Natural Gas as a Future Fuel for Heavy-Duty Vehicles". SAE Tech. Paper Series n°2001-01-2067, In: Government/Industry Meeting, Washington, D.C.

MacDonald, J. A. F. and Quinn, D. F., 1998. "Carbon Adsorbents for Natural Gas Storage". In: *Fuel*, Vol. 77, no. 1, pp. 61-64.

Moran, M. J. and Shapiro, H. N., 2000. **Fundamentals of Engineering Thermodynamics**. 4th Edition, New York, NY: John Willey & Sons, Inc.

Mota, J. P. B.; Rodrigues, A. E.; Saatdjian, E.; and Tondeur, D., 1997. "Dynamics of Natural Gas Adsorption Storage Systems Employing Activated Carbon". In: *Carbon*, V.35, n°9, pp.1259-1270.

Tien, C., 1994. **Adsorption Calculations and Modeling**. 1st Edition, Newton, MA: Butterworth-Heinemann series in chemical engineering.

Vasiliev, L. L.; Kaninchik, L. E.; Mishkinis, D. A.; and Rabetsky, M. I., 2000. "Adsorbed Natural Gas Storage and Transportation Vessels". In: *Int. J. of Thermal Sciences*, n° 39, pp. 1047-1055.

## 8. Copyright Notice

The author is the only responsible for the printed material included in his paper.